Boletim da Sociedade Astronômica Brasileira, **32**, no. 1, 101-102
© SAB 2020

Simulating the collision velocity of the dissociative galaxy cluster Abell 2034

Micheli T. Moura & Rubens E. G. Machado

[1] Universidade Tecnológica Federal do Paraná, Rua Sete de Setembro 3165, Curitiba, Brazil.
e-mail: micheli_trindade.moura@hotmail.com

Abstract. Collisions between clusters of galaxies generate disturbances in gas morphology. There are collisions that can dissociate the gas from the dark matter present in the clusters, and this is the particular case of a dissociative collision. Based on gravitational lensing analysis, it was verified that A2034 has dissociative characteristics. We aim to reconstruct the dynamic history of A2034 via numerical simulations. We executed hydrodynamic *N*-body simulations of cluster collisions represented by halos of dark matter and gas with masses similar to the virial mass, investigating different parameters and collision velocities. Preliminary results indicate that velocity is an important parameter for dissociation between gas and dark matter, therefore from a numerical analysis, it can be concluded that we are observing A2034 approximately 0.27 Gyr after the central passage, considering an initial velocity of 2000 km/s. Alternative models need to be explored to investigate different parameters that may have influence in this dissociative context.

Resumo. Colisões entre aglomerados de galáxias geram distúrbios na morfologia do gás. Existem colisões que podem dissociar o gás da matéria escura presente nos aglomerados, e esse é o caso particular de uma colisão dissociativa. Baseado na análise de lentes gravitacionais, foi verificado que A2034 possui características dissociativas. Objetivamos reconstruir a história dinâmica de A2034 via simulações numéricas. Executamos simulações numéricas de *N*-corpos de colisões entre aglomerados representados por halos de matéria escura e gás, com massas similares à massa do virial, investigando diferentes parâmetros e velocidades de colisão. Resultados preliminares indicam que a velocidade é um importante parâmetro para a dissociação entre o gás e a matéria escura, sendo assim, a partir de uma análise numérica, pode ser concluído que estamos observando A2034 aproximadamente 0.27 Gyr após a passagem central, considerando uma velocidade inicial de 2000 km/s. Modelos alternativos precisam ser explorados para investigar diferentes parâmetros que podem influenciar nesse contexto dissociativo.

Keywords. Galaxies: clusters: individual: A2034 – Galaxies: clusters: intracluster medium – Methods: numerical

1. Introduction

Galaxy clusters are the largest gravitationally bound structures in the universe, having mass on the order of $10^{14} - 10^{15}\,\mathrm{M}_\odot$. Their mass is distributed among galaxies (contributing about ~5% of the total mass), intra-cluster medium gas ~15% and dark matter, composing approximately ~80% of the total mass. Cluster formation occurs through mergers, making the collision scenario of these large structures common. The observed gas morphology of the A2034 cluster suggests a post-collision scenario (Monteiro-Oliveira, et al. 2018; Kempner, Sarazin & Markevitch 2003) given that the peak of X-ray emission is at a considerable distance from the brightest cluster galaxy (BCG). A2034 was observed by ROSAT (David, Forman & Jones 1999), ASCA (White 2000), XMM-Newton (Kempner, Sarazin & Markevitch 2003), and Chandra satellites (Owers, et al. 2014). It is at redshift $z = 0.114$ and consists of two substructures: A2034S having $M_{200}^{\mathrm{S}} = 2.35 \times 10^{14}\,\mathrm{M}_\odot$ and A2034N with $M_{200}^{\mathrm{N}} = 1.08 \times 10^{14}\,\mathrm{M}_\odot$ (Monteiro-Oliveira, et al. 2018).

2. Aims

We aim to reconstruct the dynamic history of A2034 through numerical simulations. The main constraint is to reproduce the observed morphology of the 740 kpc separation between the total mass peaks, with an X-ray peak between them (left panel of Fig. 1).

3. Methods

We use the Clustep[1] code to create initial conditions. From the virial mass of A2034, we use 15% gas mass and 85% dark matter mass to generate each cluster. For the dark matter halo distribution, we use the Hernquist (1990) profile (equation 1) in the initial condition and the Dehnen (1993) profile for the gas density (equation 2):

$$\rho_{\mathrm{h}}(r) = \frac{M_{\mathrm{dm}}}{2\pi}\,\frac{a_{\mathrm{dm}}}{(r + a_{\mathrm{dm}})^3} \tag{1}$$

$$\rho_{\mathrm{g}}(r) = \frac{3M_{\mathrm{gas}}}{4\pi}\,\frac{a_{\mathrm{gas}}}{(r + a_{\mathrm{gas}})^4}\,, \tag{2}$$

where M_{dm} represents total dark matter mass, and a_{dm} is a scale length for the Hernquist profile. Similarly, for the Dehnen profile, M_{gas} represents the total gas mass and a_{gas} is the scale length. We use the Gadget-2 (Springel 2005) code to calculate gravitational evolution of *N*-bodies and hydrodynamic interactions using SPH (Smoothed Particle Hydrodynamics). From the initial separation of 3000 kpc, we explored velocities in the range of 1000 km/s to 3000 km/s and impact parameters of 0 to 400 kpc. For the analysis and interpretation of data we use python libraries of data visualization e.g.: yt-project[2].

[1] http://github.com/ruggiero/clustep
[2] http://yt-project.org

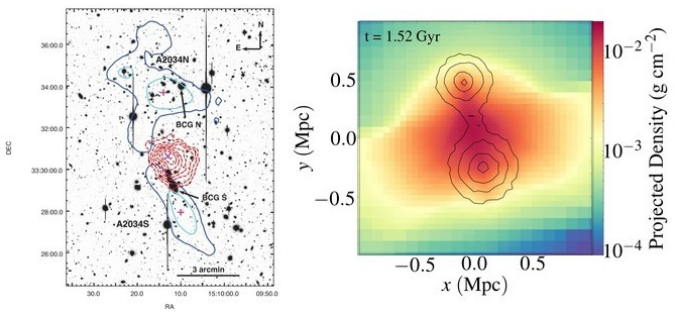

Figure 1. Left: A2034 observed in the optical. Cyan and blue curves represent total mass peaks (1 σ and 2 σ), and red curves represent X-ray emission, (Monteiro-Oliveira, et al. 2018). Right: projected gas density of A2034 at 0.27 Gyr after central passage made via numerical simulation. The contour curves represent dark matter halo distribution.

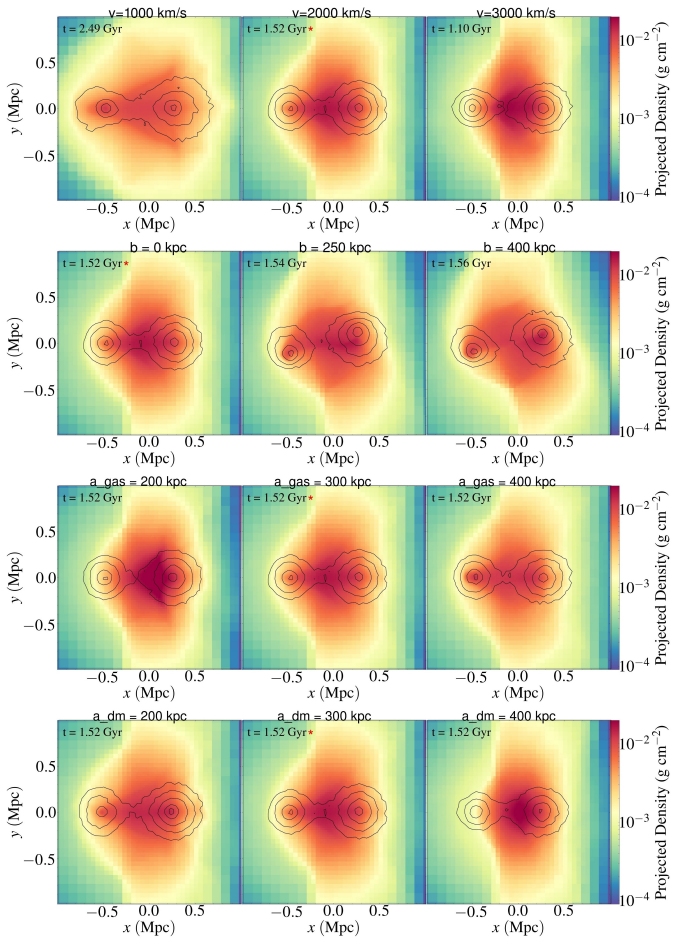

Figure 2. Projected gas density with contour curves representing dark matter halo distribution. Each row shows the results for the variation of parameters: velocity, impact parameter, scale length of gas and dark matter halo, respectively. The red "*" indicates the best model for each parameter analysed.

4. Results and discussion

To obtain the model that best represents the current features of A2034 we vary the following parameters in the simulations: initial velocity v, and impact parameter b, from initial conditions generated using different scale length $a_{\rm gas}$ and $a_{\rm dm}$ for the south substructure, keeping the northern cluster fixed at $a_{\rm gas}$ and $a_{\rm dm}$ = 200 kpc. As illustrated in Fig. 2, it is possible to notice that large impact parameters and low velocities do not present the best results for the studied cluster, considering the observational aspects. Another relevant factor that should be explored further is the gas and halo scale lenght for the both substructures. Through the preliminary analysis of initial velocity v, impact parameter b and scale lengths a parameters, it was possible to infer a model that best approximates the observational features of A2034 (observed dark matter peaks with separation of approximately 740 kpc). This comparison is made in Fig. 1. It consists of v = 2000 km/s, b = 0 kpc, and $a_{\rm gas}$ and $a_{\rm dm}$ = 300 kpc, for the cluster A2034S and $a_{\rm gas}$ and $a_{\rm dm}$ = 200 kpc for the A2034N cluster. From the best parameters analysed, it was possible construct the temporal evolution of the cluster, illustrated in Fig. 3.

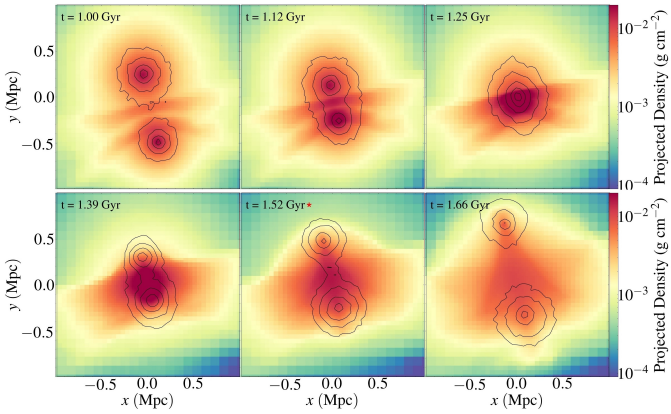

Figure 3. Temporal evolution of the projected gas density of the best model, with contour curves representing dark matter halo distribution. The frames were rotated to match the position angle of the observed cluster. The red "*" represents the instant whose separation between the dark matter peaks is 740 kpc (the best moment of the simulation) for comparison with observational data.

5. Perspectives

Future work includes refining simulations, varying scale lengths and concentration for both clusters, inclination and others parameters to obtain the best model for A2034. We aim to produce mock X-ray images to allow for a better comparison with observational data.

Acknowledgements. UTFPR & Sociedade Astrônomica Brasileira (SAB).

References

David L. P., Forman W., Jones C., 1999, ApJ, 519, 533
Dehnen W., 1993, MNRAS, 265, 250
Hernquist L., 1990, ApJ, 356, 359
Kempner J. C., Sarazin C. L., Markevitch M., 2003, ApJ, 593, 291
Kempner J. C., Sarazin C. L., Markevitch M., 2003, ApJ, 593, 291
Monteiro-Oliveira R., Cypriano E. S., Vitorelli A. Z., Ribeiro A. L. B., Sodré L., Dupke R., Mendes de Oliveira C., 2018, MNRAS, 481, 1097
Owers M. S., et al., 2014, ApJ, 780, 163
Springel V., 2005, MNRAS, 364, 1105
White D. A., 2000, MNRAS, 312, 663